SUPERFAST CONVERGENCE RATE IN ADAPTIVE ARRAYS

Anatolii A. Kononov, Chang-Ho Choi and Do-Hyung Kim
Research Center, STX Engine
Yongin-si, 16914 Korea
kaa@ieee.org; eva0307@onestx.com; d_h_kim@onestx.com

Abstract— This paper introduces a class of model-matched Toeplitz covariance matrix estimation (MM TCME) algorithms for adaptive arrays. Adaptive filters employing these algorithms are referred to as TMI filters. When the angular separation between the interference sources is not too close to a certain statistical resolution limit (SRL), the convergence rate for TMI filters is superior to that of loaded persymmetric covariance matrix inversion (LPMI) filters and to that of the well-known loaded SMI (LSMI) filters. In terms of the 3dB average SNR loss, for the TMI filters, the required training sample size is about $m/2$ (m is the number of interference sources), while that for the LPMI and LSMI filters is about m and $2m$, respectively. Since the TMI filters may suffer severe SNR degradation when the angular separation between the sources is near the SRL two remedies for dealing with this problem are discussed herein.

Keywords— adaptive array; adaptive detection; convergence rate; persymmetry; Toeplitz covariance; uniform linear array

I. INTRODUCTION

For adaptive array filters, the minimum number of training samples $N_{3\text{dB}}$ required to ensure the average signal-to-noise ratio (SNR) loss within 3dB relative to the optimal Wiener filter is accepted as the convergence measure of effectiveness [1 – 3]. It is well-known that the 3dB average SNR loss for adaptive array filters that employ the sample covariance matrix (SCM) estimator

$$\hat{\mathbf{R}} = N^{-1}(\mathbf{X}_N \mathbf{X}_N^{\text{H}}) \tag{1}$$

can be achieved if the number of training samples N meets the condition $N \geq N_{3\text{dB}} \simeq 2M$, where M is the array dimension.

In formula (1) above, the N-sample training data matrix $\mathbf{X}_N = [\mathbf{x}_1 ... \mathbf{x}_N] \in \mathbb{C}^{M \times N}$ is composed of N independent and identically distributed samples $\mathbf{x}_i \sim \mathcal{CN}(M, \mathbf{0}, \mathbf{R})$, $i = 1,\ldots,N$, having an M-variate zero-mean complex circular Gaussian distribution with common covariance matrix $\mathbf{R}$; the superscript $^{\text{H}}$ denotes the Hermitian transposition.

In most adaptive detector radar applications, the available amount of training samples is very limited [2, 3], namely $N < M$. Therefore, achieving highest convergence rate - minimizing the required training sample size $N_{3\text{dB}}$ - is one of the major problems in designing adaptive detectors.

Efficient solutions to this problem are based on taking advantage of certain favorable properties of the disturbance covariance matrix (CM) resulting from physical nature in the interference and array geometry. For instance, one of the physically adequate models of the actual (true, exact) CM $\mathbf{R}$ at the array output is given as a sum of the full rank covariance due to the white thermal noise of power σ_o^2 and a CM of a low-rank m ($m << M$) resulting from the powerful external interferences. As is well known, for this kind of low-rank (LR) structure models, the eigenspectrum of $\mathbf{R}$ comprises m dominant eigenvalues (sorted in descending order) followed by M–m equal minimum eigenvalues

$$\lambda_1 \geq \lambda_2 \geq \ldots \geq \lambda_m >> \lambda_{m+1} = \ldots = \lambda_M = \sigma_\text{o}^2. \tag{2}$$

Many adaptive detection techniques exist that rely on the LR structure property (2), see, e.g. [2 – 4] and references therein. The essential advantage of these techniques is that $N_{3\text{dB}}$ is independent of the array dimension M, and is given by

$$N_{3\text{dB}} \approx 2m, \tag{3}$$

which is a significant convergence rate improvement over well-known basic adaptive detectors [2]: sample covariance matrix inversion (SMI) detector, generalized likelihood ratio test (GLRT), adaptive matched filter (AMF), and adaptive coherence estimator (ACE), all of which require $N_{3\text{dB}} \geq 2M$.

Also note that the loaded sample covariance matrix inversion (LSMI) filter [2], employing the diagonally loaded SCM of the $\hat{\mathbf{R}}(\beta) = \hat{\mathbf{R}} + \beta\sigma_\text{o}^2\mathbf{I}$ form, with β being the real-valued loading factor, behaves as an LR method, i.e., $N_{3\text{dB}}$ for the LSMI filter is also given by (3). This behavior is analytically proven in [5] for the "cliff-like" scenarios (2).

In general, a basis of m linearly independent vectors is needed to specify the signal subspace of $\mathbf{R}$. Therefore, the lower bound for $N_{3\text{dB}}$ is assumed to be m [2]. However, as first proven in [5], the statistically justified lower bound for $N_{3\text{dB}}$ in LR interference scenarios is given by (3).

More efficient covariance estimators can be derived by incorporating, in addition to the LR structure property, information on the structure of the exact CM due to array geometry. As shown in [6], exploiting the persymmetry of the exact CM in addition to its LR structure, leads to essential performance improvement; the required sample support is

$$N_{3\text{dB}} \approx m \tag{4}$$

instead of $2m$ when only the LR property is employed.

Formula (4) can be explained by considering a specific symmetry of the eigenvectors of Hermitian persymmetric matrices. As has been shown in [7, 8], the upper $M/2$ entries in each eigenvector are equal to the reversed complex conjugate lower $M/2$ entries. Therefore, when the exact CM $\mathbf{R}$ is persymmetric, the statistical information contained in the training samples is used to estimate only M free variables, which are the unbound real and imaginary parts of entries in the m dominant (signal subspace) eigenvectors. This number of free variables is less by a factor of two than that when the LR structure of $\mathbf{R}$ is employed. Recall, if the estimator uses only the LR structure property, then $N_{3dB} \approx 2m$. Thus, if the estimator uses persymmetry in addition to the LR structure, other conditions being equal, one can expect the required training sample size to be halved, i.e., $N_{3dB} \approx m$.

All Toeplitz matrices are persymmetric; hence, their eigenvectors also possess the specific symmetry property described above. Moreover, the eigenvectors of Hermitian Toeplitz matrices possess another kind of symmetry such that the imaginary part in any eigenvector is just its reversed real part [8]. Thus, in case of the Toeplitz CM, the number of free variables to be estimated is reduced by a factor of two in addition to the reduction resulting from the persymmetry. In this case, one can, therefore, assume that the statistically justified N_{3dB} can be evaluated as

$$N_{3\text{dB}} \approx m/2\,. \tag{5}$$

The purpose of this paper is to introduce a class of Toeplitz covariance estimation algorithms and to demonstrate that for adaptive TMI filters that employ these algorithms the required sample support agrees to that predicted by (5).

II. Problem Formulation

Consider a uniform linear array (ULA) of M sensors with inter-sensor spacing $d/\lambda = 0.5$, where λ is the wavelength determined by a common center frequency of m external far-field sources that radiate continuous narrow-band plane waves simultaneously impinging upon the array.

We model the Gaussian processes in the array as a mixture of the white thermal noise of power $p_0 = \sigma_0^2$ and m interfering signals having the directions of arrival (DOAs) $\boldsymbol{\theta} = [\theta_1,...,\theta_m]$ (or $\mathbf{u} = [u_1,...,u_m]$, $u_k = \sin\theta_k$) and powers $\mathbf{p} = [p_1,..., p_m]$. The interfering signals and thermal noise are assumed to be uncorrelated. Under these conditions, the exact CM at the array output can be written as a structured model as follows

$$\mathbf{R} = \sum_{k=1}^{m} p_k \mathbf{s}(u_k)\mathbf{s}^{\mathrm{H}}(u_k) + p_0\mathbf{I}\,, \tag{6}$$

where $\mathbf{s}(u_k) = [1, e^{j\pi u_k},..., e^{j\pi(M-1)u_k}]^{\mathrm{T}}$ is the $M\times 1$ array steering vector corresponding to the kth source, $k = 1, \ldots, m$.

The model-matched (MM) covariance matrix estimator is defined as identical to (6), where $\mathbf{R}$ is substituted with an estimate $\hat{\mathbf{R}}_{\mathrm{T}}$ (the subscript T denotes the Toeplitz matrix) and the unknown parameters are substituted with their corresponding estimates $\hat{m}$, $\hat{p}_{\mathrm{o}}$, $\hat{\mathbf{u}}$ and $\hat{\mathbf{p}}$.

Since all Toeplitz matrices are persymmetric and because exploiting the persymmetry reduces N_{3dB} from $2m$ to m, to get more accurate estimates of the DOA $u_1, \ldots, u_m$ and powers $p_1, \ldots, p_m$, it is reasonable to use the known persymmetric estimate [6] instead of the SCM (1) with MUSIC, Root MUSIC, SSMUSIC or another appropriate DOA estimator. Having obtained accurate estimates of m and p_{o}, we can then compute a final estimate of the actual CM by substituting the estimates into the MM estimator.

If positive definite Toeplitz CM estimates from the MM estimator are accurate enough, then due to the two intrinsic properties of the eigenvectors of Toeplitz matrices discussed above, this estimator can be expected to ensure the 3dB SNR loss even if the sample support is as small as that given by (5).

III. Toeplitz CM Estimation Algorithm

To improve the performance of DOA and power estimators, we substitute the generic SCM (1) with the persymmetric estimate of the true Toeplitz CM. Substitution allows using some unitary transformations [7, 8] that convert the true complex CM into a real-valued one, thereby giving the algorithm the advantage of real-valued data processing [9]. In the case of Toeplitz CM, this type of processing can also be had by using appropriate unitary transformations. We use the unitary transformations given by the matrices

$$\mathbf{U}_{\mathrm{P}} = \frac{1}{\sqrt{2}}\begin{bmatrix} \mathbf{I}_2 & \mathbf{J}_2 \\ j\,\mathbf{I}_2 & -j\mathbf{J}_2 \end{bmatrix};\quad \mathbf{U}_{\mathrm{T}} = \frac{1}{\sqrt{2}}[\mathbf{I} - j\mathbf{J}]\,, \tag{7}$$

where $\mathbf{U}_{\mathrm{P}}$ and $\mathbf{U}_{\mathrm{T}}$ represents unitary transformation for persymmetric and Toeplitz CM, respectively. While $\mathbf{I}_2$ and $\mathbf{J}_2$ respectively, represent the identity and exchange matrix, of dimension $M/2$ (we consider only the even M case), $\mathbf{I}$ and $\mathbf{J}$ respectively, represent the identity and exchange matrix of dimension M.

The persymmetric estimate of the exact CM $\mathbf{R}$ is directly obtained from the SCM $\hat{\mathbf{R}}$ as [6, 10]

$$\hat{\mathbf{R}}_{\mathrm{RP}} = \mathrm{Re}(\mathbf{U}_{\mathrm{P}}\hat{\mathbf{R}}\mathbf{U}_{\mathrm{P}}^{\mathrm{H}})\,, \tag{8}$$

where the subscript RP means that $\hat{\mathbf{R}}_{\mathrm{RP}}$ is a symmetric matrix representing the persymmetric CM estimate.

An exemplary MM TCME algorithm is summarized below as *Main Algorithm*. This algorithm employs three auxiliary algorithms A1, A2, and A3. Algorithms A1 and A2 assume that p_{o} is an arbitrary constant from an *a priori* known interval, i.e., $p_{\mathrm{o}} \in [p_{\mathrm{o1}}, p_{\mathrm{o2}}]$, $p_{\mathrm{o1}} < p_{\mathrm{o2}}$. Making allowances for estimation errors the interval $[\gamma_{\mathrm{LB}} p_{\mathrm{o1}}, \gamma_{\mathrm{UB}} p_{\mathrm{o2}}]$ is assigned to be used by algorithm A1 as a check interval in initial rank estimation where $\gamma_{\mathrm{LB}} < 1$ and $\gamma_{\mathrm{UB}} > 1$ are defined assuming that only thermal noise is present (see Section 4).

Main Algorithm. Model-Matched TCME Algorithm

1. Given N and $\mathbf{X}_N = [\mathbf{x}_1 \ldots \mathbf{x}_N]$ obtain matrix $\hat{\mathbf{R}}$ by (1).
2. Compute matrix $\hat{\mathbf{R}}_{\mathrm{RP}}$ by (8).
3. For matrix $\hat{\mathbf{R}}_{\mathrm{RP}}$, obtain its eigenvalues $|\hat{\lambda}_1| \geq |\hat{\lambda}_2| \geq \ldots \geq |\hat{\lambda}_M|$ and corresponding eigenvectors $\hat{\mathbf{e}}_k$, $k = 1, 2, \ldots, M$.
4. Use algorithm A1 to compute initial estimate $\hat{m}_{\mathrm{in}}$.
5. Use algorithm A2 to compute initial estimate $\hat{p}_{\mathrm{oin}}$.
6. If $\hat{m}_{\mathrm{in}} = 0$, then compute Toeplitz covariance estimate as $\hat{\mathbf{R}}_{\mathrm{T}} = \hat{p}_{\mathrm{oin}}\mathbf{I}$ and stop; otherwise go to step 7.
7. Use algorithm A3 to compute final fine estimates of DOAs and powers $\hat{u}_{k_1}$, $\hat{u}_{k_2}$, …, $\hat{u}_{k_{\hat{m}}}$ and $\hat{p}_{k_1}$, $\hat{p}_{k_2}$, …, $\hat{p}_{k_{\hat{m}}}$, respectively, and final estimates $\hat{m}$ and $\hat{p}_{\mathrm{o}}$.
8. Compute positive definite Toeplitz CM estimate as

$$\hat{\mathbf{R}}_{\mathrm{T}} = \sum_{i=1}^{\hat{m}} \hat{p}_{k_i} \mathbf{s}(\hat{u}_{k_i}) \mathbf{s}^{\mathrm{H}}(\hat{u}_{k_i}) + \hat{p}_{\mathrm{o}} \mathbf{I} \quad . \qquad (9)$$

Algorithm A1. Estimation of Number of Sources

1. If the number of sources m is known, then $\hat{m}_{\mathrm{in}} = m$ and stop; otherwise go to step 2.
2. Compute $P_\lambda = \sum_{k=1}^{M} |\hat{\lambda}_k|$ and $\mu = P_\lambda / M$.
3. If $\mu \in [\gamma_{\mathrm{LB}} p_{\mathrm{o1}}, \gamma_{\mathrm{UB}} p_{\mathrm{o2}}]$, then $\hat{m}_{\mathrm{in1}} = 0$ and go to step 4, otherwise define $k_{\max}$ as such a maximum index $k = 1, 2, \ldots, M$, for which $|\hat{\lambda}_k|/P_k > T_\lambda$, where T_λ is a predefined threshold, and then compute $\hat{m}_{\mathrm{in1}} = \min(k_{\max}, M-1)$.
4. Use SORTE algorithm [11, p. 2010] to compute $\hat{m}_{\mathrm{in2}}$.
5. Compute initial estimate of the number of sources as

$$\hat{m}_{\mathrm{in}} = \lceil \alpha_m \hat{m}_{\mathrm{in1}} + (1-\alpha_m)\hat{m}_{\mathrm{in2}} \rceil,$$

where α_m is the predefined weighting coefficient.

Algorithm A2. Noise Power Estimation

1. If the noise power $p_{\mathrm{o}} = \sigma_{\mathrm{o}}^2$ is known, then $\hat{p}_{\mathrm{oin}} = p_{\mathrm{o}}$ and stop; otherwise go to step 2.
2. Compute $\eta = \sum_{k=\hat{m}_{\mathrm{in}}+1}^{M} |\hat{\lambda}_k| / (M - \hat{m}_{\mathrm{in}})$
3. If $\eta \in [\gamma_{\mathrm{LB}} p_{\mathrm{o1}}, \gamma_{\mathrm{UB}} p_{\mathrm{o2}}]$, then $\hat{p}_{\mathrm{oin}} = \eta$; otherwise if $\eta < \gamma_{\mathrm{LB}} p_{\mathrm{o1}}$, then $\hat{p}_{\mathrm{oin}} = p_{\mathrm{o1}}$; else $\eta > \gamma_{\mathrm{UB}} p_{\mathrm{o2}}$ and then $\hat{p}_{\mathrm{oin}} = p_{\mathrm{o2}}$.

Algorithm A3. Computing final fine estimates of DOAs and powers of interference sources and final estimates of the number of sources and noise power.

1. Compute complex eigenvectors $\hat{\mathbf{v}}_k$ by transforming the eigenvectors $\hat{\mathbf{e}}_k$ as $\hat{\mathbf{v}}_k = \mathbf{U}_{\mathrm{P}}^{\mathrm{H}} \hat{\mathbf{e}}_k$, $k = 1, \ldots, M$.
2. Generate noise subspace matrix as $\hat{\mathbf{U}}_{\mathrm{NS}} = [\, \hat{\mathbf{v}}_{\hat{m}_{\mathrm{in}}+1} \ldots \hat{\mathbf{v}}_M \,]$ and then use it with Root MUSIC algorithm to compute fine DOA estimates as $\hat{u}_k = \mathrm{angle}(\hat{z}_k)/\pi$, $k = 1, 2, \ldots, \hat{m}_{\mathrm{av}}$ using $\hat{m}_{\mathrm{av}}$ = min($\hat{m}_{\mathrm{in}}, \hat{m}_{\mathrm{R}}$) roots $\hat{z}_k$ with maximum modules $|\hat{z}_k|$; these $\hat{m}_{\mathrm{av}}$ roots are selected out of $\hat{m}_{\mathrm{R}}$ roots $\hat{z}_n$ that are identified as all those roots for which $|\hat{z}_n| \le 1$ & $\mathrm{Im}(\hat{z}_n) \ne 0$.
3. Generate signal subspace matrix as $\hat{\mathbf{V}}_{\mathrm{SS}} = [\hat{\mathbf{v}}_1 \, \hat{\mathbf{v}}_2 \ldots \hat{\mathbf{v}}_{\hat{m}_{\mathrm{av}}}]$ and then use it with the power estimator from the SSMUSIC algorithm [12, p. 1384] to compute fine estimates of the powers of sources $\hat{p}_k, k = 1, \ldots, \hat{m}_{\mathrm{av}}$

$$\underset{k=1,\ldots,\hat{m}_{\mathrm{av}}}{\hat{p}_k} = \left[\sum_{n=1}^{\hat{m}_{\mathrm{av}}} \left| \mathbf{s}^{\mathrm{H}}(\hat{u}_k) \hat{\mathbf{F}}_{\mathrm{SS}}(:,n) \right|^2 \right]^{-1},$$

where $\mathbf{s}(\hat{u}_k) = [1, e^{j\pi \hat{u}_k}, e^{j\pi 2\hat{u}_k}, \ldots, e^{j\pi(M-1)\hat{u}_k}]^{\mathrm{T}}$ is the array steering vector corresponding to the k th direction of arrival $\hat{\theta}_k$ ($\hat{u}_k = \sin\hat{\theta}_k$), and the matrix $\hat{\mathbf{F}}_{\mathrm{SS}} = \hat{\mathbf{V}}_{\mathrm{SS}} \hat{\mathbf{\Lambda}}_{\mathrm{SS}}^{-1/2}$ with $\hat{\mathbf{\Lambda}}_{\mathrm{SS}}^{-1/2}$ being the $\hat{m}_{\mathrm{av}}$ -by- $\hat{m}_{\mathrm{av}}$ diagonal matrix

$$\hat{\mathbf{\Lambda}}_{\mathrm{SS}}^{-1/2} = \mathrm{diag}[(|\hat{\lambda}_k| - \hat{p}_{\mathrm{oin}})^{-1/2}, \, k = 1, \ldots, \hat{m}_{\mathrm{av}}].$$

4. Define all indices k that $\hat{p}_k > \alpha_{\mathrm{D}} \hat{p}_{\mathrm{oin}}$, $k = 1, \ldots, \hat{m}_{\mathrm{av}}$, where α_{D} is the predefined constant used in computing the threshold for detecting actual peaks due to interference sources. Let $k_1, k_2, \ldots, k_{\hat{m}}$ be the set of survived indices. The total number of survived indices $\hat{m}$ is the final estimate of the number of sources m. Final fine estimates of DOAs and powers are $\hat{u}_{k_1}, \ldots, \hat{u}_{k_{\hat{m}}}$ and $\hat{p}_{k_1}, \ldots, \hat{p}_{k_{\hat{m}}}$, respectively.
5. Compute the final noise power estimate $\hat{p}_{\mathrm{o}}$ using algorithm A2 with $\hat{p}_{\mathrm{o}}$ and $\hat{m}$ instead of $\hat{p}_{\mathrm{oin}}$ and $\hat{m}_{\mathrm{in}}$, respectively.

IV. Performance Analysis

This section compares the convergence performance in terms of the average SNR loss for the following adaptive filters: the conventional LSMI filter, the diagonally loaded persymmetric matrix inversion (LPMI) filter that exploits the estimate (8) plus $(\beta\hat{p}_{\mathrm{o}})\mathbf{I}$ term, and the Toeplitz matrix inversion (TMI) filter based on the noniterative MM TCME algorithm proposed in the present paper (*Main Algorithm*). Respectively, the filter weight vectors are:

$$\mathbf{w}_{\mathrm{LSMI}} = \hat{\mathbf{R}}(\beta)^{-1} \mathbf{s}_{\mathrm{t}}, \qquad (10)$$

$$\mathbf{w}_{\mathrm{LPMI}} = \hat{\mathbf{R}}_{\mathrm{RP}}(\beta)^{-1} \mathbf{s}_{\mathrm{Pt}}, \qquad (11)$$

$$\mathbf{w}_{\mathrm{TMI}} = \hat{\mathbf{R}}_{\mathrm{RT}} \mathbf{s}_{\mathrm{Tt}}. \qquad (12)$$

In (10) – (12) above, $\mathbf{s}_{\mathrm{Pt}} = \mathbf{U}_{\mathrm{P}} \mathbf{s}_{\mathrm{t}}$ and $\mathbf{s}_{\mathrm{Tt}} = \mathbf{U}_{\mathrm{T}} \mathbf{s}_{\mathrm{t}}$, where $\mathbf{s}_{\mathrm{t}}$ is the normalized ($\mathbf{s}_{\mathrm{t}}^{\mathrm{H}} \mathbf{s}_{\mathrm{t}} = 1$) array-signal steering vector for a target from a given direction θ_{t}, the matrices in (10) and (11) are $\hat{\mathbf{R}}(\beta) = \hat{\mathbf{R}} + (\beta\hat{p}_{\mathrm{o}})\mathbf{I}$ and $\hat{\mathbf{R}}_{\mathrm{RP}}(\beta) = \hat{\mathbf{R}}_{\mathrm{RP}} + (\beta\hat{p}_{\mathrm{o}})\mathbf{I}$, respectively, and the symmetric CM estimate $\hat{\mathbf{R}}_{\mathrm{RT}}$ in (12) is computed from (9) as

$$\hat{\mathbf{R}}_{\mathrm{RT}} = \mathrm{Re}(\mathbf{U}_{\mathrm{T}} \hat{\mathbf{R}}_{\mathrm{T}} \mathbf{U}_{\mathrm{T}}^{\mathrm{H}}). \qquad (13)$$

The SNR loss factor ρ_{AF}, where AF stands for one of the abbreviated names of the filters under study, is given by

$$\rho_{\mathrm{AF}} = \frac{|\mathbf{v}_{\mathrm{AF}}^{\mathrm{H}} \mathbf{s}_{\mathrm{t}}|^2}{(\mathbf{v}_{\mathrm{AF}}^{\mathrm{H}} \mathbf{R} \, \mathbf{v}_{\mathrm{AF}})(\mathbf{s}_{\mathrm{t}}^{\mathrm{H}} \mathbf{R}^{-1} \mathbf{s}_{\mathrm{t}})}, \qquad (14)$$

where the new weight vector $\mathbf{v}_{\mathrm{AF}}$ is defined as: $\mathbf{v}_{\mathrm{AF}} = \mathbf{w}_{\mathrm{LSMI}}$ for the LSMI filter (i.e., if AF = LSMI), $\mathbf{v}_{\mathrm{AF}} = \mathbf{U}_{\mathrm{P}}^{\mathrm{H}} \mathbf{w}_{\mathrm{LPMI}}$ if AF = LPMI, and $\mathbf{v}_{\mathrm{AF}} = \mathbf{U}_{\mathrm{T}}^{\mathrm{H}} \mathbf{w}_{\mathrm{TMI}}$ if AF = TMI.

In all examples here, a ULA of $M = 12$ sensors, a Hamming weighted steering vector $\mathbf{s}_{\mathrm{t}}$ tuned to $\theta_{\mathrm{t}}=0$ (providing a quiescent array pattern with –39 dB sidelobes), parameter $\beta = 2$ as in (10) and (11), and N_{MC} = 4,000 Monte-Carlo trials are used. Before statistical trials, a fixed noise power value p_{o} is generated as a random quantity uniformly distributed on the interval $[p_{\mathrm{o1}}, p_{\mathrm{o2}}] = [1, 4]$.

Fig. 1 plots the average SNR loss factor for a Root MUSIC-based TMI filter: this is an adaptive filter employing the MM TCME algorithm with Root MUSIC being a fine DOA estimator (Algorithm A3, step 2). In subsequent examples, we

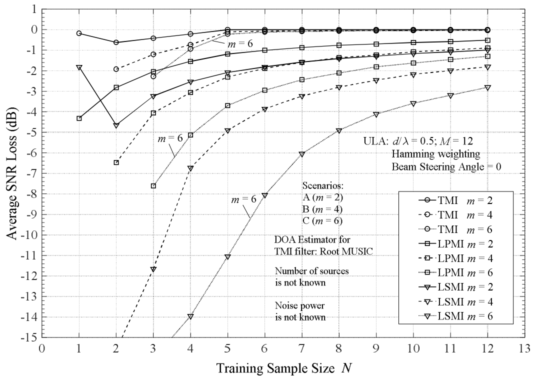

Fig. 1. Average SNR loss factor versus N for Root MUSIC-based TMI filter in Scenarios A, B and C, m is unknown

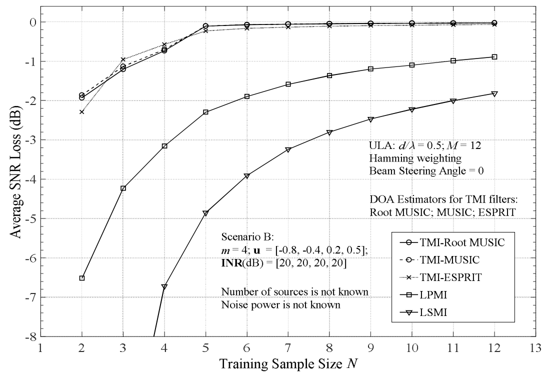

Fig. 2. Convergence performance comparison for adaptive filters under study; Scenario B, m is unknown

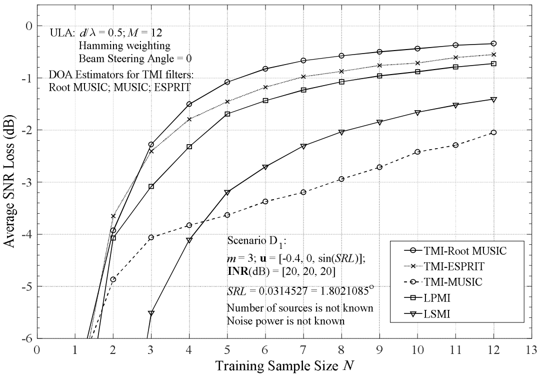

Fig. 3. Convergence performance comparison for adaptive filters under study; Scenario D_1, m is unknown

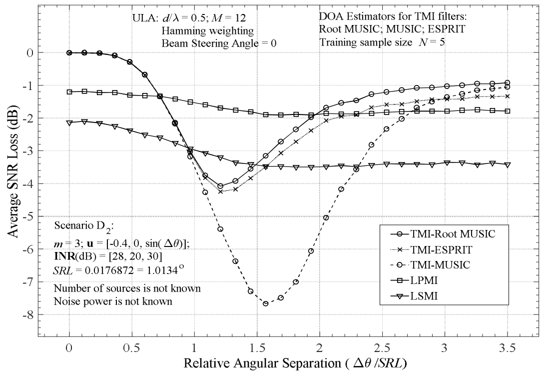

Fig. 4. Average SNR loss factor versus $\Delta\theta/SRL$ for adaptive filters under study; Scenario D_2, m is unknown, $N = 5$

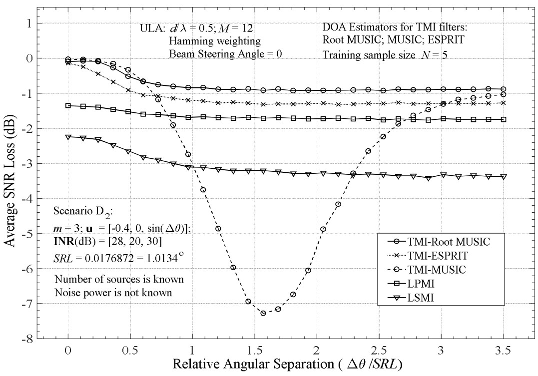

Fig. 5. Average SNR loss factor versus $\Delta\theta/SRL$ for adaptive filters under study; Scenario D_2, m is known, $N = 5$

compare the performance of the Root MUSIC-based TMI filter with that of the ESPRIT/MUSIC-based TMI filter.

If only white thermal noise is present, the noise power estimate μ (see algorithm A1) will have a gamma distribution dependent on M, N, and p_o. The coefficients $\gamma_{LB} = 0.3081$ and $\gamma_{UB} = 2.2846$ are computed from the conditions $\Pr\{\mu \le \gamma_{LB} p_{o1}\} = \delta$ and $\Pr\{\mu \le \gamma_{UB} p_{o2}\} = 1 - \delta$, for $\delta = 10^{-6}$, if the actual noise power is $p_{o1} = 1$ and $p_{o2} = 4$, respectively, $M = 12$ and $N = 2$.

As an approximate "balance point," the settings $T_\lambda = 0.0075$ and $\alpha_m = 0.9$ are empirically found using a MUSIC-based TMI filter in high interference-to-noise ratio (INR) Scenario B (see below) for fixed $\alpha_D = 2$ and $p_o = 1$. The search intervals for T_λ and α_m are defined as [0.001, 0.01] and [0.5, 0.999], respectively. Departure from this "balance point" in either direction does not lead to noticeable improvement in average SNR loss factor simultaneously either in high INR Scenario B or low INR Scenario B with INR = 5 dB for all the sources.

Fig. 1 shows the average values of ρ_{LSMI}, ρ_{LPMI}, and ρ_{TMI} versus N (averaged over N_{MC} = 4,000 Monte-Carlo trials) in Scenario A $\{m = 2, \mathbf{u} = [-0.8, -0.4], \text{INR}=p_1/p_o=p_2/p_o=100\}$, in Scenario B $\{m = 4, \mathbf{u} = [-0.8, -0.4, 0.2, 0.5], \text{INR}=p_1/p_o=...=p_4/p_o= 100\}$, and in Scenario C $\{m = 6, \mathbf{u} = [-0.8, -0.4, 0.2, 0.5, 0.7, 0.9], \text{INR (dB)} = 10\lg(p_k/p_o) = 20, k = 1, 2, \dots, m\}$. Both the noise power and the number of sources are assumed to be unknown.

In all these scenarios, the sources are well-separated in the angular coordinate. By the well-separated interference sources, we understand the sources with such the smallest angular separation between them that is not too close to the statistical resolution limit (SRL) [13]. In this paper, we define the SRL as

$$SRL = \frac{0.5\,FRL}{(SNR_{\text{arr}})^{1/4}}, \tag{15}$$

where $FRL = 2\pi/M$ is the standard Fourier resolution limit and $SNR_{\text{arr}} = 4 \cdot M \cdot SNR_{\text{elt}}$ is the array SNR with SNR_{elt} being the element-level SNR.

Fig. 1 confirms that $N_{3\text{dB}}$ for the TMI filter agrees with the prediction in (5), i.e., $N_{3\text{dB}}$ = 1, 2 and 3 for Scenarios A, B, and C with m = 2, 4 and 6, respectively. For the LSMI and LPMI filters, $N_{3\text{dB}}$ is also in accord with the predictions given by (3) and (4), respectively.

Fig. 2 compares the performance of the Root MUSIC-based TMI filter with that of the MUSIC-based TMI filter and the ESPRIT-based TMI filter in high INR Scenario B. The curves in Fig. 2 show that all the TMI filters under study exhibit similar convergence performance in a scenario with well-separated sources. In Scenario B, the smallest angular separation is 18.4630° (0.3222 rad), between the third and fourth sources. The absence of the performance degradation in Fig. 2 allows concluding that this separation is not too close to the SRL value SRL = 1.80211° (0.0314527 rad) calculated from (15) for $SNR_{\text{elt}} = \max(\text{INR}_3, \text{INR}_4) = 20$ dB.

However, the convergence performance of TMI filters may severely degrade when the angular separation between sources is near the SRL. Fig. 3 plots the average SNR loss factors in Scenario D_1 {$m = 3$, $\mathbf{u}=[-0.4, 0.0, \sin(\Delta\theta)]$, $p_1/p_o = p_2/p_o = p_3/p_o = 100$} when the smallest angular separation $\Delta\theta = SRL$ = 1.80211° (0.0314527 rad). It is assumed that both the noise power and the number of interference sources are not known. As can be seen in Fig. 3, an essential drop in the output SNR occurs for the MUSIC-based TMI filter, while the performance of the Root MUSIC-based TMI filter and that of the ESPRIT-based TMI filter are quite robust.

This SNR degradation results from the well-known MUSIC performance breakdown [14] when DOA estimates generated by MUSIC contain outliers due to closely spaced sources. The method proposed in [14] can be effective in detecting the presence of outliers what is needed to rectify DOA estimates by using known "performance breakdown cure" procedure [15].

Next, we consider an unfavorable scenario in which the performance of the Root MUSIC-based TMI filter and that of the ESPRIT-based TMI filter may decline. Fig. 4 demonstrates how these filters degrade in Scenario D_2 {$m = 3$, $\mathbf{u} = [-0.4, 0.0, \sin(\Delta\theta)]$, **INR** (dB) = [28, 20, 30]} under the condition that both p_o and m are not known. In this scenario, the statistical resolution limit SRL = 1.0134° (0.0176872 rad) for $SNR_{\text{elt}} = \max(\text{INR}_2, \text{INR}_3) = 30$dB. Fig. 4 shows the average SNR loss factor as a function of the relative angular separation $\Delta\theta/SRL$ for $N = 5$. As can be seen, the performance degradation takes place for all the filters under study. However, the performance of the Root MUSIC-based filter is rather better relative to that of other filters.

To eliminate possible detrimental effect from output SNR degradation in the TMI filters, we will propose an efficient solution in the framework of two-stage adaptive detection [2] in our next paper submitted to this conference. This solution will be based on a joint scalar CFAR detection rule for the individual AMF detectors employing the LPMI and TMI filters.

In the same Scenario D_2, Fig. 5 plots the curves like those presented in Fig. 4 under the assumption that the number of sources m is known (rank-constrained scenario). As can be seen, the MUSIC-based TMI filter collapses for $0.8SRL \leq \Delta\theta \leq 2.7SRL$, while the Root MUSIC/ESPRIT-based TMI filters are robust independently of the angular separation.

V. CONCLUSION

In this paper, we have presented a class of model-matched Toeplitz covariance matrix estimation (MM TCME) algorithms for adaptive arrays. Each algorithm in this class includes a set of techniques for estimating the noise power, the number of interference sources, the DOAs and powers of sources. This class may incorporate any combination of the listed types of estimators that enhance the performance of the TMI filters.

We have introduced an exemplary noniterative MM TCME algorithm (*Main Algorithm*) that uses known estimation techniques, particularly, the Root MUSIC algorithm and the power estimator from the SSMUSIC algorithm.

The novelty of the MM TCME algorithms arises from their capability to ensure superfast conversion rate. As has been shown, in scenarios with well-separated interference sources, the adaptive TMI filters employing the introduced exemplary MM TCME algorithm are superior to the LPMI and LSMI filters. For the TMI filters, the required training sample size is about $m/2$, while that for the LPMI and LSMI filters is about m and $2m$, respectively.

In our next paper submitted to this conference, we will show that new rapidly adaptive CFAR detectors, which we will design within the framework of a two-stage adaptive detection paradigm by merging individual two-stage AMF detectors which use the LPMI and TMI filters, are free of performance degradation due to possible output SNR drop in TMI filters.

Finally, an important observation has been made that the number of free variables in dominant eigenvectors of the exact covariance matrix is an essential parameter determining the required training sample size in adaptive filters. Monte-Carlo simulations confirm this statement for all the filters under study.

REFERENCES

[1] I.S. Reed, J.D. Mallett, and L.E. Brennan, "Rapid convergence rate in adaptive arrays," IEEE Trans. AES, vol. 10, no. 6, pp. 853–863, November 1974.

[2] Maio, A.D., and M.S. Greco (Eds.), Modern Radar Detection Theory, Chapter 6, SciTech Publishing, Edison, NJ, 2016.

[3] M. Steiner and K. Gerlach, "Fast converging adaptive processor for a structured covariance matrix," IEEE Trans. AES, vol. 36, no. 4, pp. 1115–1126, October 2000.

[4] C.D. Peckham, A.M. Haimovich, T.F. Ayoub, et al., "Reduced-rank STAP Performance analysis," IEEE Trans. AES, vol. 36, no. 2, pp. 664–676, April 2000.

[5] O. Cheremisin, "Efficiency of adaptive algorithms with regularized sample covariance matrix," Radio Eng. Electron. Phys., vol. 27, no. 10, pp. 69–77, 1982.

[6] G. Ginolhac, P. Forster, F. Pascal and J.P. Ovarlez, "Exploiting persymmetry for low-rank space time adaptive processing," Signal Processing, Elsevier, vol. 97, no. 4, pp. 242–251, 2014.

[7] M.J. Goldstein, "Reduction of the eigenproblem for Hermitian persymmetric matrices," Math. Computation, vol. 28, no. 125, pp. 237–238, January 1974.

[8] D.M. Wilkes, S.D. Morgera, F. Noor, and M.H. Hayes, III, "A Hermitian Toeplitz matrix is unitarily similar to a real Toeplitz-plus-Hankel matrix," IEEE Trans. SP, vol. 39, no. 9, pp. 2146–2148, September 1991

[9] D.A. Linebarger, R.D. DeGroat and E.M. Dowling, "Efficient direction-finding methods employing forward/backward averaging," IEEE Trans. SP, vol. 42, no. 8, pp. 2136–2145, August 1994.

[10] G. Pailloux, P. Forster, J.P. Ovarlez, and F. Pascal, "Persymmetric adaptive radar detectors," IEEE Trans. AES, vol. 47, no. 4, pp. 2376–2390, October 2011.

[11] Z. He, A. Cichocki, S. Xie and K. Choi, "Detecting the number of clusters in *n*-way probabilistic clustering," IEEE Trans. PA and MI, vol. 32, no. 11, pp. 2006–2021, November 2011.

[12] M.L. McCloud and L.L. Scharf, "A new subspace identification algorithm for high-resolution DOA estimation," IEEE Trans. AP, vol. 50, no. 10, pp. 1382–1390, October 2002.

[13] S.T. Smith, "Statistical resolution limits and the complexified Cramér-Rao bound," IEEE Trans. SP, vol. 53, no. 5, p. 1602, May 2005.

[14] Y.I. Abramovich and B.A. Johnson, "GLRT-based detection-estimation for undersampled training conditions," IEEE Trans. SP, vol. 56, no. 8, pp. 3600–3612, August 2008.

[15] M. Hawkes, A. Nehorai, and P. Stoica, "Performance breakdown of subspace-based methods: Prediction and cure," in Proceedings of the IEEE ICASSP, Salt Lake, UT, vol. 6, pp. 4005–4008, 2001.